Ray propagation in nematic droplets

J. A. Reyes*
Liquid Crystal Institute, Kent State University, Kent, Ohio 44242
(Received 6 October 1997; revised manuscript received 3 February 1998)

We present a model for the propagation of optical beams in a nematic droplet. For a low intensity electromagnetic field, we first derive an analytical asymptotic expression for the configuration of a nematic droplet that satisfies hard-anchoring, bipolar boundary conditions. Then, from Maxwell's equation, we find the corresponding eikonal equation valid in the limit of geometrical optics. From the latter equation we find the ray trajectories for the radial and bipolar configurations for various sets of initially parallel rays, and show how they are deflected by a nematic droplet. We also find the presence of caustics and return points, whose positions depend on the initial conditions. Finally, we summarize our results. [S1063-651X(98)15605-2]

PACS number(s): 42.70.Df, 78.20.Fm, 42.79.Kr

I. INTRODUCTION

Light propagation in birefringent inhomogeneous media is a difficult problem which has been extensively studied in the last years for planar geometries. In fact, for the case of a plane wave and layered media, different procedures have been used for solving this problem. One of the most widely utilized methods in liquid crystals is that of Barreman's [1] 4×4 matrix formalism which was shown to be equivalent to Maxwell's equation for linear propagation. Some other approaches based on the well known geometrical optics approximation have been also applied to describe beam propagation in planar geometries [2,3]. Electromagnetic modes have been considered for certain cylindrical geometries by using either numerical procedures [4] or the so called WKB approximation [5].

The development of polymer-dispersed liquid crystals (PDLC's), which are dispersions of liquid crystal rich droplets in a polymer matrix [6], has brought about a great deal of interest in the study of light propagation in spherical geometries. The size of spherical droplets in these materials is usually uniform but can vary between 0.1 and 10 μm. The nematic configuration within droplets depends on surface anchoring and elastic constants, and is responsible for the refractive and birefringent properties of the droplets. It should be mentioned that the electro-optic properties of PDLC's are among the reasons for their potential applicability in different devices [7,8].

There have been some pioneering works [9,10] devoted to analyzing light scattering from a nematic droplet. Two complementary physical limits were considered in these works, namely, the Rayleigh-Gans approximation and the anomalous-diffraction approach, which assume, respectively, a much smaller and much larger droplet radius than the wavelength of the light; also, both of these suppose a small dielectric anisotropy. For the latter work, these assumptions allowed the author to consider the light as a ray which does not change its direction but only suffers a change of phase; that is to say, the refractive effects which stem from the local changes of the refraction index induced by the nematic configuration are completely neglected. These refractive effects are expected to be important in birefringent and inhomogeneous media like liquid crystals even for moderate dielectric anisotropy values, and are able to curve the trajectory of light beams as well as induce local changes of phase instead of global changes, which can develop in richer diffraction patterns.

The purpose of this paper is to study this refractive effect by analyzing the dynamics of transverse modes which propagate in a nematic droplet, in the limit of geometrical optics. More specifically, we shall calculate and analyze the ray trajectories for both the radial and bipolar configurations, as well as some other physical parameters involved.

To this end this paper is organized as follows. In Sec. II we deduce, from Frank's energy density, an asymptotic analytical expression for the bipolar configuration. In Sec. III we derive the eikonal equation in a nematic droplet from Maxwell's equation, in the limit of geometrical optics. In Sec. IV we calculate the ray trajectories for the radial and bipolar configurations by using analytical and numerical procedures. Finally, Sec. V is devoted to summarizing our work and presenting our results.

II. BIPOLAR CONFIGURATION

We consider a spherical nematic droplet of radius R which satisfies the hard-anchoring bipolar boundary conditions [11] (see Fig. 1). We will consider a coordinate system whose origin is at the center of the droplet, and for which the bipolar axis is parallel to the z axis. Then, if θ is the polar angle of the spherical coordinates and $\hat{n}$ is the nematic director, the bipolar boundary condition is given by $\hat{n}(r=R,\theta)=\hat{e}_\theta$, where $\hat{e}_\theta$ is the unit vector in the direction of increasing θ. One may express the director in terms of the angle ψ, measured from $\hat{e}_\theta$ and contained in the plane defined by this vector and $\hat{e}_r$, where $\hat{e}_r$ is the unit vector in the direction of increasing r; that is,

$$\hat{n}=\sin\psi(r,\theta)\hat{e}_r+\cos\psi(r,\theta)\hat{e}_\theta, \tag{2.1}$$

where we have used the azimuth symmetry of this nematic configuration. Note that the boundary condition given by Eq. (2.1) imposes on ψ the condition $\psi(r=R,\theta)=0$.

*On leave from Instituto de Física, UNAM, México, Distrito Federal, Mexico.

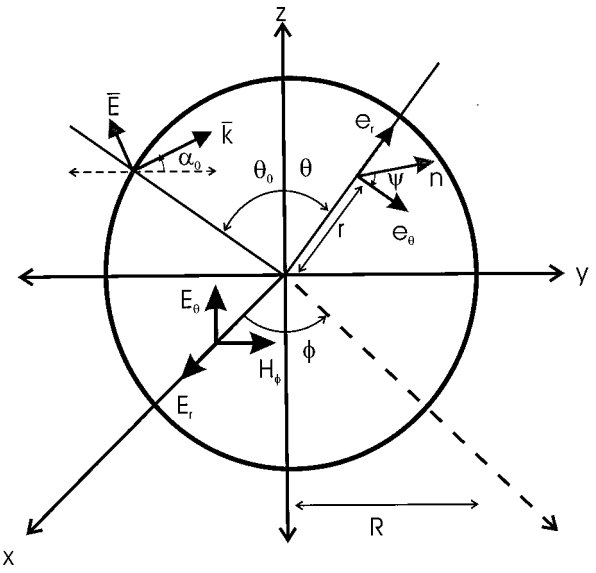

FIG. 1. Diagram of a nematic droplet where the nematic director and the transverse magnetic modes are shown.

A nematic liquid crystal confined to a small spherical volume, where the surface-to-volume ratio is relatively high, exhibits a specific nematic configuration resulting from the elastic forces. For droplets whose radii R are larger than $R>100$ nm, surface-induced changes in the nematic order parameter can be neglected [12], and thus the nematic director $\hat{n}$ can be determined by minimizing Frank's free energy, that in the equal elastic constant approximation $K\equiv K_1=K_3$ can be written [13]

$$\mathcal{F}=(RK/2)\int_V d\theta\, d\phi\, dt\, \sin\theta e^t\left[\left(\frac{\partial\psi}{\partial t}\right)^2+\left(\frac{\partial\psi}{\partial\theta}\right)^2+3\sin^2\psi+1+\cot^2\theta\cos^2\psi+\sin 2\psi\frac{\partial\psi}{\partial t}-2(\sin^2\psi+1)\frac{\partial\psi}{\partial\theta}+2\frac{\partial\psi}{\partial t}\cot\theta\cos^2\psi+2\sin 2\psi\cot\theta-\sin 2\psi\cot\theta\frac{\partial\psi}{\partial\theta}\right], \tag{2.2}$$

where V is the droplet volume and $t=\ln(r/R)$. Thus the configuration equation is obtained by calculating the variational derivative of Eq. (2.2) with respect to ψ, leading to

$$\frac{\partial^2\psi}{\partial t^2}+\frac{\partial^2\psi}{\partial\theta^2}+\frac{\partial\psi}{\partial t}+\cot\theta\frac{\partial\psi}{\partial\theta}-\sin 2\psi+\frac{\sin 2\psi}{2\sin^2\theta}-\cot\theta\cos 2\psi-\cot\theta=0. \tag{2.3}$$

Now we look for a solution for Eq. (2.3) of the form $\tan\psi=\kappa(t)\cot\theta$, where $\kappa(t)$ is an arbitrary function of t which satisfies the boundary conditions $\kappa(t=1)=0$ and $\kappa(t=-\infty)=-1$. Here the first condition comes from $\psi(r=R)=0$, and the second one guarantees the continuity of ψ at the center. The reasons for choosing this kind of solution are first, $\hat{n}(\theta=0,\pi,\pi/2)=-\hat{k}$ for any $\kappa(t)$, where $\hat{k}$ is the unit vector along the z axis. This means that $\hat{n}$ is parallel to $-\hat{k}$ along the z axis ($\theta=0,\pi$) and on the equator plane ($\theta=\pi/2$), which is the expected behavior for this configuration. Second, it can be shown that this expression describes asymptotically the solution of Eq. (2.3) near its poles. Substitution of $\tan\psi=\kappa(t)\cot\theta$ into Eq. (2.3), yields

$$\frac{d^2\kappa}{dt^2}+\frac{d\kappa}{dt}+\frac{-2\kappa\left(\frac{d\kappa}{dt}\right)^2\cos^2\theta+2\kappa(1-\kappa^2)}{\sin^2\theta+\kappa^2\cos^2\theta}-2\kappa-2=0. \tag{2.4}$$

In general, Eq. (2.4) is not consistent because κ depends only on t; hence we integrate Eq. (2.4) with respect to θ from 0 to π; this leads to

$$r^2\frac{d^2\kappa}{dr^2}+2r\frac{d\kappa}{dr}+2r^2\frac{\left(\frac{d\kappa}{dr}\right)^2}{1-\kappa}-2(\kappa+1)(2-\kappa)=0. \tag{2.5}$$

By using the shooting method, we numerically calculate the solution of Eq. (2.5), for a 50-μm droplet, that satisfies the corresponding boundary conditions; this is shown in Fig. 2. In order to provide a simple analytical expression for the configuration, that will be useful in the following sections, we shall approximate $\kappa(r)\approx r/R-1$. Hence $\hat{n}$ can be obtained by inserting $\tan\psi=(r/R-1)\cot\theta$ into Eq. (2.1); we arrive at

$$\hat{n}=\frac{z\rho\hat{e}_\rho+(\rho^2-\sqrt{z^2+\rho^2})\hat{k}}{\sqrt{\rho^2(\sqrt{z^2+\rho^2}-1)^2+z^2}}, \tag{2.6}$$

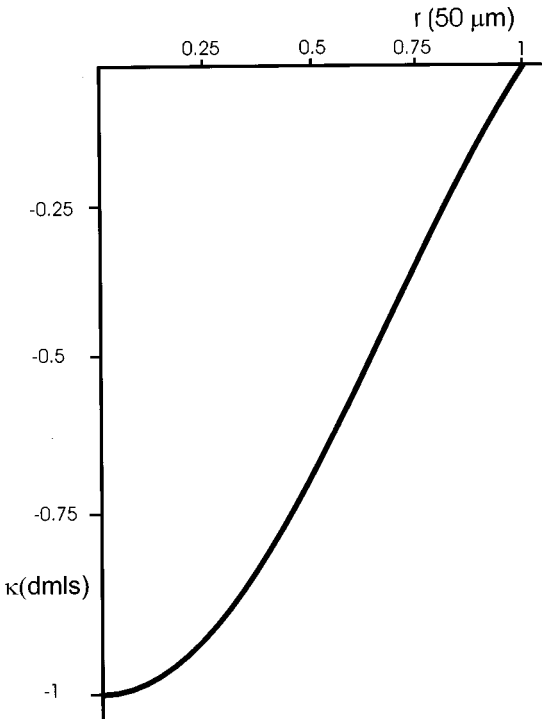

FIG. 2. Numerical solution of Eq. (2) satisfying boundary conditions $\kappa(r=R=50\ \mu\text{m})=0$ and $\kappa(r=0)=-1$ $\kappa(r)$ is a dimensionless (dmls) function defined in Sec. II.

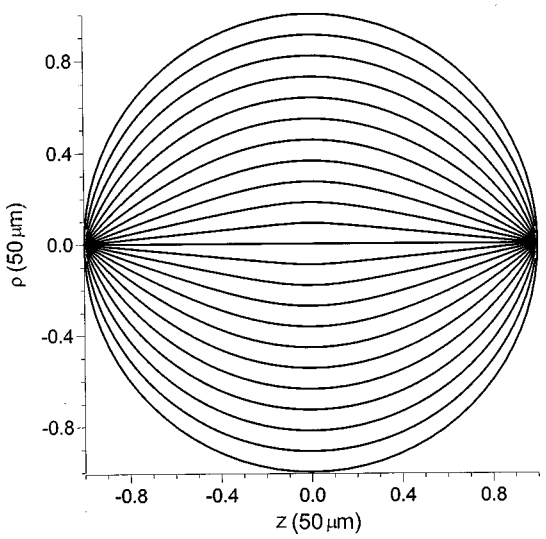

FIG. 3. Director lines for various equally separated initial condition at the equator plane.

where $z=r\cos\theta$ and $\rho=r\sin\theta$ are the cylindrical coordinates, and $\hat{e}_\rho$ is the unit vector in the increasing direction of ρ. To show this nematic's configuration graphically, we define the director lines in the following way:

$$\frac{d\rho}{dz}=\frac{n_\rho}{n_z}=\frac{z\rho}{\rho^2-\sqrt{z^2+\rho^2}}. \tag{2.7}$$

Thus $\hat{n}$ is parallel to the curve which passes through the point where $\hat{n}$ is to be calculated. Figure 3 plots some of the curves given by Eq. (2.7), which are drawn equally separated at the equator plane ($z=0$).

III. GEOMETRICAL OPTICS

We shall restrict our analysis to consider electromagnetic fields, $\vec{\mathcal{E}}$ and $\vec{\mathcal{H}}$ whose z component of angular momentum $\hat{l}_z=i\hbar\,d/d\phi$ vanishes, that is, $\hat{l}_z\vec{\mathcal{E}}=\hat{l}_z\vec{\mathcal{E}}=0$. This means physically that the wave vector associated with these fields lies in the plane generated by $\hat{e}_r$ and $\hat{e}_\theta$. The propagation of these waves within a nematic droplet can be described in terms of the representation provided by the corresponding TM and TE modes, which have the components $\mathcal{H}_\phi$, $\mathcal{E}_r$, and $\mathcal{E}_\theta$ and $\mathcal{E}_\phi$, $\mathcal{H}_r$, and $\mathcal{H}_\theta$, respectively. Notice that for both the radial and bipolar configuration, which can be expressed by Eq. (2.1), the TE modes are not coupled to θ because their only electric component is parallel to $\hat{e}_\phi$. As a result, they cannot induce a torque on $\hat{n}$. Thus in the rest of this section we shall ignore them. The monochromatic TM modes for our system are given by

$$\mathcal{H}_\phi(r,\theta,t)=e^{i\omega t}H_\phi(r,\theta,k_0) \tag{3.1}$$

and

$$\mathcal{E}_{r,z}(r,\theta,t)=e^{i\omega t}E_{r,z}(r,\theta,k_0), \tag{3.2}$$

where $E_\theta(r,\theta,k_0)$, $E_r(r,\theta,k_0)$, and $H_\phi(r,\theta,k_0)$ are the TM amplitudes, $k_0=\omega/c$ is the free space wave number, and m is an integer number. Here ω is the frequency of the field and c the speed of light in vacuum.

Using Maxwell's equations without sources to describe the optical field within the liquid crystal, we arrived at the following general set of equations for the amplitudes of the TM modes ($x\equiv r/R$):

$$\frac{1}{x}\frac{\partial}{\partial x}\left(\epsilon_{rr}\frac{\partial}{\partial x}(xH_\phi)+\frac{\epsilon_{r\theta}}{\sin\theta}\frac{\partial}{\partial\theta}(\sin\theta H_\phi)\right)+\frac{1}{x^2}\frac{\partial}{\partial\theta}\left(\epsilon_{r\theta}\frac{\partial}{\partial x}(xH_\phi)+\frac{\epsilon_{\theta\theta}}{\sin\theta}\frac{\partial}{\partial\theta}(\sin\theta H_\phi)\right)+\epsilon_\perp\epsilon_\parallel k_0^2R^2H_\phi=0, \tag{3.3}$$

$$E_r=-\frac{i}{\epsilon_\perp\epsilon_\parallel k_0Rx}\left\{\frac{\epsilon_{\theta\theta}}{\sin\theta}\frac{\partial}{\partial\theta}(\sin\theta H_\phi)+\epsilon_{r\theta}\frac{\partial}{\partial x}(xH_\phi)\right\}, \tag{3.4}$$

$$E_\theta=\frac{i}{\epsilon_\perp\epsilon_\parallel k_0Rx}\left\{\frac{\epsilon_{r\theta}}{\sin\theta}\frac{\partial}{\partial\theta}(\sin\theta H_\phi)+\epsilon_{rr}\frac{\partial}{\partial x}(xH_\phi)\right\}, \tag{3.5}$$

and where $\epsilon_\parallel$ and $\epsilon_\perp$ denote, respectively, the dielectric constants parallel and perpendicular to the long axis of the molecules. $\epsilon_a=\epsilon_\parallel-\epsilon_\perp$ is the dielectric anisotropy of the nematic and the components of the dielectric tensor; $\epsilon_{ij}=\epsilon_\perp\delta_{ij}+\epsilon_a n_i n_j$ are explicit functions of θ and x, namely, $\epsilon_{rr}=\epsilon_\perp+\epsilon_a\sin^2\psi(x,\theta)$; $\epsilon_{\theta\theta}=\epsilon_\perp+\epsilon_a\cos^2\psi(x,\theta)$; and $\epsilon_{r\theta}=\epsilon_{\theta r}=\epsilon_a\sin\psi(x,\theta)\cos\psi(x,\theta)$.

We can approximate Eqs. (3.3)–(3.5) by supposing a low intensity incident beam whose optical wavelength is much smaller than the droplet radius, so that $1/k_0R\ll1$. The former condition guarantees that ψ is not distorted by the electromagnetic field, and the latter condition defines the well known limit of geometrical optics [14]. Following the usual procedure in geometrical optics [15], we assume the following form for the TM mode components:

$$H_\phi(x,\theta,k_0)=H_{0\phi}\exp[i(k_0RW(x,\theta)-\omega t)] \tag{3.6}$$

Here $W(x,\theta)$ is the characteristic function of Hamilton, which is equal to the difference in optical paths of a ray propagating between two fixed point in the droplet. The amplitudes $H_{0\phi}$ and E_{0j} are general complex functions of the position. Substitution of Eq. (3.6) into Eq. (3.3), by keeping terms up to order zero in $1/k_0R$, leads to

$$\epsilon_{rr}\left(\frac{\partial W}{\partial x}\right)^2+2\frac{\epsilon_{r\theta}}{x}\left(\frac{\partial W}{\partial\theta}\right)\left(\frac{\partial W}{\partial x}\right)+\frac{\epsilon_{\theta\theta}}{x^2}\left(\frac{\partial W}{\partial\theta}\right)^2=\epsilon_\perp\epsilon_\parallel. \tag{3.7}$$

This equation is the so-called eikonal or Hamilton-Jacobi equation.

IV. RAY TRAJECTORIES

We will study the ray propagation for the radial and the bipolar nematic droplet configurations by using the TM mode formalism developed in Sec. III.

A. Radial configuration

The radial configuration can be represented by Eq. (2.1) if taking $\psi=\pi/2$; hence for this configuration Eq. (3.7) does not depend explicitly on θ, so that we can separate this variable by using the canonical transformation $W=P(x)-q_0\theta$, where $P(x)$ is a function which depends only on x, and q_0 is the angular momentum which is conserved. Thus W is given by

$$W=-q_0\theta+\left[\epsilon_\perp\left(x^2-\frac{q_0^2}{\epsilon_\parallel}\right)\right]^{1/2}+q_0\left(\frac{\epsilon_\parallel}{\epsilon_\perp}\right)^{1/2}\arccos\left[\frac{q_0}{x\sqrt{\epsilon_\parallel}}\right]+P_0, \tag{4.1}$$

where P_0 is an integration constant. According to the Hamilton-Jacobi theory, the ray trajectory is given by $\gamma=\partial W(x,\theta,q_0)/\partial q_0$, where γ is the variable conjugated to q_0, which is invariant in time; that is, an initial condition or constant of motion. It leads to

$$r=\frac{q_0R/\sqrt{\epsilon_\parallel}}{\cos[\sqrt{\epsilon_\parallel/\epsilon_\perp}(\theta-\gamma)]}. \tag{4.2}$$

Now, both q_0 and γ can be expressed in terms of the initial θ_0 and incidence α_0 angles at the sphere border: $r=R=50$ μm (see Fig. 1). We use the following general relation, which can be derived from the coordinate transformation $z=r\cos\theta$ and $\rho=r\sin\theta$:

$$\tan\alpha=\frac{\cos\theta-r\dfrac{d\theta}{dr}\sin\theta}{\sin\theta+r\dfrac{d\theta}{dr}\cos\theta}, \tag{4.3}$$

where $\tan\alpha_0=dz/d\rho$. Then, substituting θ from Eq. (4.2) into Eq. (4.3) by taking $x=1$, leads to

$$q_0=\frac{\sqrt{\epsilon_\parallel}\cos(\alpha_0+\theta_0)}{\sqrt{(\epsilon_\perp/\epsilon_\parallel)\sin^2(\alpha_0+\theta_0)+\cos^2(\theta_0+\alpha_0)}} \tag{4.4}$$

and

$$\gamma=\theta_0-\left(\frac{\epsilon_\perp}{\epsilon_\parallel}\right)^{1/2}\arccos\left[\frac{q_0}{\sqrt{\epsilon_\parallel}}\right]. \tag{4.5}$$

Some optical quantities can be calculated from Eq. (4.2). First, the return point of the trajectory is obtained by setting $\theta=\gamma$, because r reaches its minimum value $r_r=q_0(\theta_0+\alpha_0)R/\sqrt{\epsilon_\perp}$. Note that $r_r=0$ at normal incidence $\beta=\theta_0+\alpha_0-\pi/2=0$, and $r_r\to1$ when $\beta=\pi/2$ tends to $\pi/2$, as should be expected. Second, since W is itself the optical path of the trajectory, we directly obtain the change of phase of the ray $\Delta f=[W(r=R)-W(r=r_r)]/2\pi$ in crossing the whole droplet, by substituting θ from Eq. (4.2) into Eq. (4.1); we arrive at $\Delta f=(\sqrt{\epsilon_\perp}/\pi)\cos\beta/\sqrt{\cos^2\beta+(\epsilon_\parallel/\epsilon_\perp)\sin^2\beta}$. Note that for $\beta=0$, ΔW has its maximum value, and this is the same as in an isotropic medium, which means that the ray propagates in a straight line at normal incidence and ΔW tends to 0 when $\beta\to\pi/2$, as should be expected.

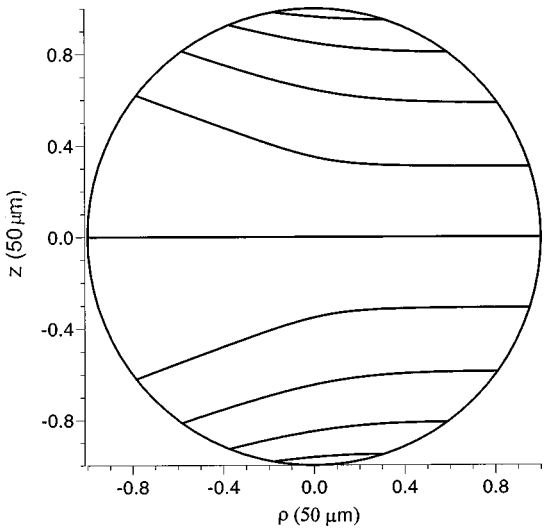

FIG. 4. Ray trajectories, for the radial configuration, starting from the right, initially parallel to each other and with equally separated values of θ_0, namely, $\theta_0=\pm\pi/8$, $\pm\pi/4$, ... and $\pm\pi/2$; for the incident angle $\alpha_0=0$. We use a typical nematic cyanobiphenil for which $\epsilon_\perp=2.25$ and $\epsilon_\parallel=2.89$.

The form of the trajectories can be inferred from Eq. (4.2). Notice that all the trajectories are symmetric with respect to the angle γ, thus the angle θ_s over the sphere surface at which the ray comes out is given by the condition $\theta_s-\gamma=-(\theta_0-\gamma)$, and then $\theta_s-\theta_0=2(\gamma-\theta_0)$. In fact, from Eq. (4.5), we note that the maximum and minimum angles allowed for θ_s are $\theta_0\pm\sqrt{\epsilon_\perp/\epsilon_\parallel}\pi/2$. Thus, besides the normal incident ray whose ray trajectory is a straight line that crosses the center, as was shown above, every ray cannot reach a dark zone delimited by the angle $\pi(1-\sqrt{\epsilon_\perp/\epsilon_\parallel})$ which lies behind the droplet. That is to say, there is a defocusing effect that makes the droplet behave as a divergent lens.

In Fig. 4, we plot rays which start from the right, are initially parallel to each other, and are equally separated over the sphere border; for the incident angles, $\alpha_0=0$. Here we are considering a 50-μm nematic droplet for which $\epsilon_\perp=2.25$ and $\epsilon_\parallel=2.89$. This figure shows how the rays diverge from the equator plane in such a way that the rays nearer to the equator are bent more than the rays which lie further from it. The same behavior is expected for any value of α because of the symmetry of the configuration. In Fig. 5, we plot a set of rays with the same θ_0 and various values of α; this graph shows clearly the presence of the dark zone induced by the droplet.

We should mention that if we want to follow a plane wave which comes from outside the droplet, we have to take into account the change of direction of the rays given by the Snell law at the interface droplet host. Roughly speaking, the effect of this border refraction is to add an initial divergent deflection angle to each ray, so that the dark zone mentioned above still would be present, but enhanced because the rays are to be even more scattered.

It is important to remark that because of the symmetry of the configuration, for any incident ray, it is always possible

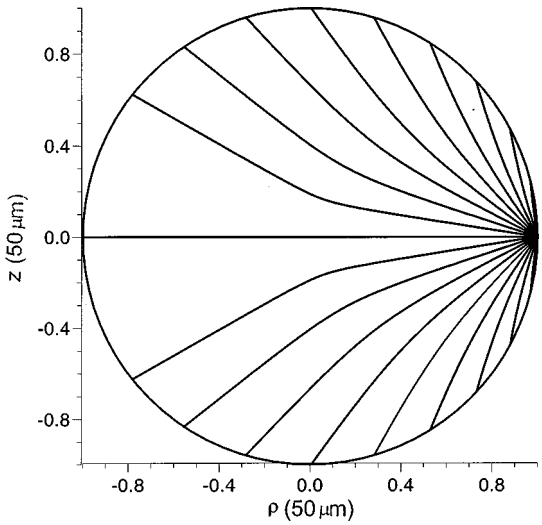

FIG. 5. Ray trajectories, for the same configuration and substance as Fig. 4, starting from the same point θ_0 for various equally separated values of α_0, namely, $\alpha=$, 0, $\pm\pi/20$, $\pm\pi/10$, ..., and $\pm 9\pi/20$.

to find a reference coordinate for which the z component of the angular momentum $\hat{l}_z = i\hbar\, d/d\phi$ vanishes. In this sense, the results for this configuration are quite general.

B. Bipolar configuration

Due to the fact that the dielectric tensor components for the bipolar configuration depend on both r and θ, we cannot solve Eq. (3.7) by separating variables as we did in Sec. IV A. However, it is well known that a first order partial equation of two independent variables can be transformed into an equivalent set of four first order ordinary differential equations, by using Charpit's equations [17], which are a generalization of the Hamilton's equations [16]. This yields

$$\frac{\epsilon_\parallel \epsilon_\perp}{R}\frac{dr}{dW} = p\,\epsilon_{rr} + \frac{\epsilon_{r\theta}}{r}\,qR, \tag{4.6}$$

$$\frac{\epsilon_\parallel \epsilon_\perp}{R}\,r\,\frac{d\theta}{dW} = p\,\epsilon_{r\theta} + \frac{\epsilon_{\theta\theta}}{r}\,qR, \tag{4.7}$$

$$\begin{aligned} 2\,\epsilon_\parallel \epsilon_\perp \frac{dq}{dW} = {} & \frac{\epsilon_a (r/R-1)}{[\sin^2\theta + (r/R-1)^2\cos^2\theta]^2} \\ & \times\left\{ \sin 2\theta\left(p^2 - \frac{q^2R^2}{r^2}\right) + \frac{2pqR}{r} \right. \\ & \left. \times[\sin^2\theta - (r/R-1)^2\cos^2\theta]\right\}, \end{aligned} \tag{4.8}$$

and

$$p = -\frac{\epsilon_{r\theta}}{r\,\epsilon_{rr}}\,qR + \frac{\sqrt{\epsilon_\perp \epsilon_\parallel (\epsilon_{rr} r^2 - q^2R^2)}}{r\,\epsilon_{rr}}. \tag{4.9}$$

Here $p = R(\partial W/\partial r)$ and $q = \partial W/\partial\theta$ are known as the radial and angular ray components. Using the Maxwell relation $R(\partial\theta/\partial r)_q = -(\partial p/\partial q)_r$, we find, from Eq. (4.9), that

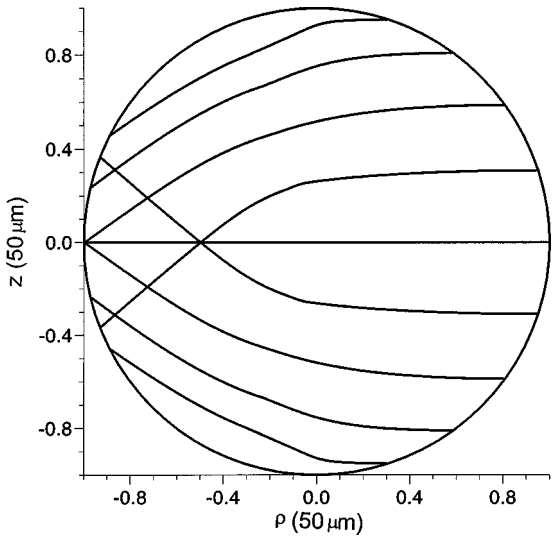

FIG. 6. Ray trajectories for the bipolar configuration starting from the right, initially parallel to each other and with equally separated values of θ_0, namely, $\theta_0 = \pm\pi/8$, $\pm\pi/4$, ..., and $\pm\pi/2$; for the incident angle $\alpha_0 = 0$. We use the same substance values as Fig. 4.

$$r\,\frac{d\theta}{dr} = \frac{qR\sqrt{\epsilon_\perp \epsilon_\parallel}}{\epsilon_{rr}\sqrt{r^2\epsilon_{rr} - q^2R^2}} + \frac{\epsilon_{r\theta}}{\epsilon_{rr}}. \tag{4.10}$$

To express q_0, the initial condition for q, in terms of α_0 and θ_0 at the droplet border (see Fig. 1), we set $r=R$ in Eq. (4.10), and insert this into Eq. (4.3). We find that q_0 is given by

$$q_0 = \frac{\sqrt{\epsilon_\perp}\,\cos(\theta_0+\alpha_0)}{\sqrt{(\epsilon_\parallel/\epsilon_\perp)\cos^2(\theta_0+\alpha_0) + \sin^2(\theta_0+\alpha_0)}}. \tag{4.11}$$

Because θ_0 and α_0 range from 0 to π and from $-\pi/2$ to $\pi/2$, respectively, this expression shows that the values of q_0 are in the interval defined by $|q| \leqslant \sqrt{\epsilon_\perp}$. It is important to point out that for $q \neq 0$, Eq. (4.10) diverges at $r^2\epsilon_{rr} - q^2R^2 = 0$, and the ray trajectory does not exist for smaller values of $x^2\epsilon_{rr}$.

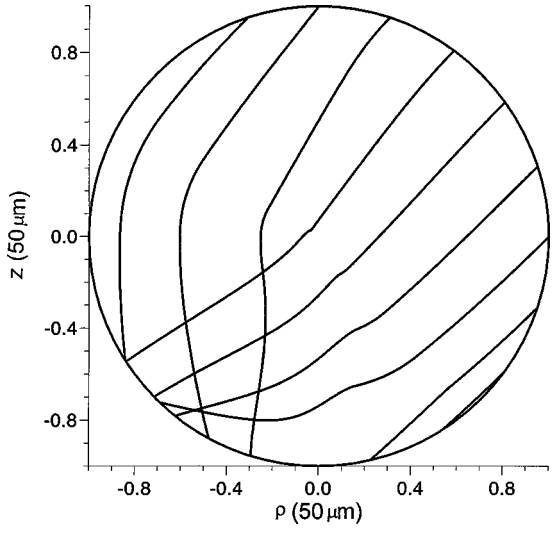

FIG. 7. The same as Fig. 6, but for $\alpha_0 = \pi/4$.

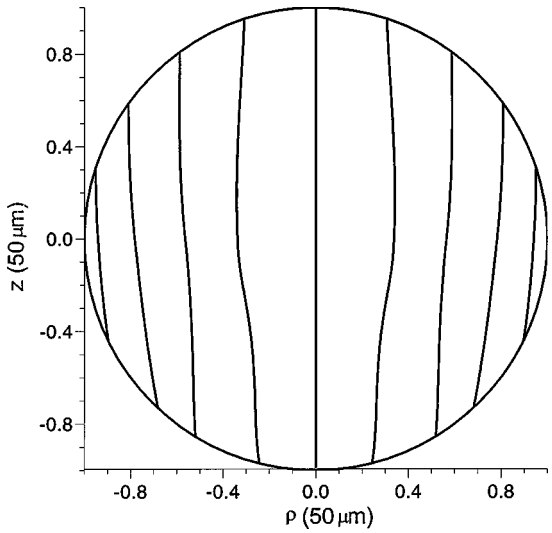

FIG. 8. The same as Fig. 7, but for $\alpha_0=\pi/2$.

In fact, this equation defines the geometrical place of the caustic for a given q_c which can be written explicitly as

$$\cos\,\theta=\left(\frac{q_c^2R^2-r^2\epsilon_\perp}{(r/R-1)^2(\epsilon_\parallel r^2-q_c^2R^2)+q_c^2R^2-\epsilon_\perp r^2}\right)^{1/2}. \tag{4.12}$$

Note that a point on this curve (return point) also satisfies $\tan\alpha_c\cot\theta_c=-1$ which comes from Eq. (4.3). This expression means that at the return point the trajectory slope is perpendicular to the corresponding polar radius.

We calculated various sets of ray trajectories for distinct initial conditions by solving Eqs. (4.6)–(4.9) numerically, and plotted them. In Figs. 6–8 we plot, for five incident angles α_0 between 0 and $\pi/2$, various sets of rays which start from the right, which are initially parallel to each other and with equally separated values of the θ_0 sphere border.

Figure 6 shows rays which are initially perpendicular to the z axis ($\alpha=0$), but are deflected by the droplet in such a way that they converge in a region on the equator. In Figs. 7 and 8, the incidence angles α_0 are larger in increasing order. Notice that the deflected ray trajectories in Fig. 8 converge to a region that lies underneath the equator plane. In contrast, Fig. 8 shows rays that are almost straight lines, for which their deflection angles are small. This means that just in the case when the incident beams are parallel to the bipolar axis, the anomalous-diffraction approach assumed in some previous work [9] is reliable.

It is interesting to remark that this formalism also provides a phase difference associated with each of the ray trajectories, since these are parametrized by W, which is itself the optical path. With this information is possible to analyze diffraction patterns.

V. CONCLUDING REMARKS

In summary, we calculated an analytical asymptotic and very simple expression for the bipolar configuration from Frank's free energy. By applying the limit of geometrical optics to the TM mode equation in nematic droplets, we derived the eikonal equation. We found analytical expressions for the optical path, ray trajectory, deflection angle, and return point for the radial configuration. We showed that an initially parallel set of incident rays is scattered by a droplet with the radial configuration, in such a way that there exists a dark zone behind the sphere unreachable for almost every ray. We numerically calculated the ray trajectories for the bipolar configuration, and showed, for various initially parallel sets of rays, that the rays are bent in such a way so as to converge in certain regions of the sphere. We hope that this work on refractive effects in nematic droplets can be useful in understanding the propagation of beams in birefringent inhomogeneous media, as well as in the design of PDLC devices.

ACKNOWLEDGMENTS

The author is indebted to Professor Jack R. Kelly for enlightening discussions. This work was supported in part by the NSF under ALCOM Grant No. BMR89-20147.

[1] D. W. Barreman, J. Opt. Soc. Am. **62**, 502 (1972).
[2] C. Oldano, Phys. Rev. A **40**, 6014 (1989).
[3] E. Santamato and Y. R. Shen, J. Opt. Soc. Am. A **4**, 356 (1987).
[4] H. Lin, P. Pallfy-Muhoray, and M. A. Lee, Mol. Cryst. Liq. Cryst. **204**, 180 (1991); H. Lin and P. Pallfy-Muhoray, Liq. Cryst. **14**, 1977 (1993); H. Lin and P. P. Pallfy-Muhoray, Opt. Lett. **17**, 722 (1992); H. Lin and P. Pallfy-Muhoray, *ibid.* **19**, 436 (1994).
[5] J. A. Reyes and R. F. Rodríguez, Opt. Commun. **134**, 349 (1997).
[6] J. W. Doane, N. A. Vaz, B.-G. Wu, and S. Zumer, Appl. Phys. Lett. **48**, 269 (1986); J. W. Doane, MRS Bull. **16**, 22 (1991).
[7] M. Schadt, Liq. Cryst. **14**, 73 (1993).
[8] H. S. Kitzerov, Liq. Cryst. **16**, 1 (1994).
[9] S. Zumer and J. W. Doane, Phys. Rev. A **34**, 3373 (1986).
[10] S. Zumer, Phys. Rev. A **37**, 4006 (1988).
[11] E. Santamato, B. Daino, M. Romagnoli, M. Settembre, and Y. R. Shen, Phys. Rev. Lett. **64**, 1377 (1990); G. Abbate, P. Maddalena, L. Marrucci, L. Saetta, and E. Santamato, J. Phys. II **1**, 543 (1991).
[12] D. W. Allender, G. L. Henderson, and D. L. Jhonson, Phys. Rev. A **24**, 1086 (1981).
[13] F. C. Frank, Faraday Discuss. Chem. Soc. **25**, 119 (1958).
[14] M. Born and E. Wolf, *Principles of Optics* (Pergamon, New York, 1975).
[15] R. Lunenburg, *Mathematical Theory of Optics* (University of California Press, Berkeley, 1964).
[16] H. Goldstein, *Classical Mechanics*, 2nd ed. (Addison-Wesley, Reading, MA, 1980), Sec. 10.3.
[17] I. N. Sneddon, *Partial Differential Equations* (McGraw-Hill, New York, 1957), Sec. 2.10.